

Axial anomaly and the triality symmetry of leptons and hadrons

Sadataka Furui

Faculty of Science and Engineering, Teikyo University

1-1 Toyosatodai, Utsunomiya, 320-8551 Japan *

February 25, 2022

Abstract

We apply the supersymmetric model of É. Cartan to the pseudoscalar meson decay into two photons, $\pi_0 \rightarrow \gamma\gamma$, $\eta \rightarrow \gamma\gamma$ and $\eta' \rightarrow \gamma\gamma$. In the book of É. Cartan published in 1966, Dirac spinors ${}^t(A, B)$ and ${}^t(C, D)$ and vector fields E and E' were introduced and five supersymmetric transformations $G_{23}, G_{12}, G_{13}, G_{123}$ and G_{132} were considered.

The Pauli spinor is treated as a quaternion and the Dirac spinor is treated as an octonion. In the pseudoscalar meson decay, when the two final vector fields belong to the same group (EE or $E'E'$), we call the diagram rescattering diagram. When they belong to different groups (EE'), the diagram is called twisted diagram.

Assuming the triality selection rules of octonions, dark matter is interpreted as matter emitting photons in a different triality sector than that of electromagnetic probes in our world.

**E-mail address:* furui@umb.teikyo-u.ac.jp

1 Introduction

According to Hawking and Mlodinow, physical theories are assembly of mathematical models or assembly of rules that connect elements of models and observables[1]. In QED, complex numbers and quaternion are used and in QCD also the same number system is used. A quaternion operates on a two-component spinor. Pauli spinor is a two-component spinor, but Dirac spinor is a four component spinor, and there is an octonion that operates on a four component spinor, which has the triality symmetry.

In the low-energy world there are two kinds of Dirac spinors, leptons e, μ and τ , and quarks u, d and s . Quarks have three-color degrees of freedom. When color degrees of freedom is large, the quark loop degrees of freedom $U(1)$ -anomaly due to difference of masses of e, μ and τ is suppressed, but in the infrared there appears quark condensates $\langle 0|\bar{q}q|\rangle \neq 0$, and $U(1)$ symmetry is broken and there appears η' meson in addition to $\pi^\pm, \pi^0, K^\pm, K^0, \bar{K}_0$ and η , that plays essential roles[2].

The anomaly was accounted for in the effective theory by the Wess-Zumino-Witten term[3, 4] and the effective Lagrangian in the presence of external source

$$\begin{aligned}\mathcal{L}_{QCD} = & \mathcal{L}_{QCD}^0 + \bar{q}\gamma_\mu(v^\mu + \gamma_5 a^\mu)q - \bar{q}(s - i\gamma_5 p)q \\ & - \frac{g^2}{16\pi^2}\theta \epsilon^{\alpha\beta\lambda\mu} tr_c(G_{\alpha\beta}G_{\mu\nu})\end{aligned}\quad (1)$$

with the vacuum angle θ was introduced in[5], and studied for a study of the mixing of η and η' [6, 7, 8, 9, 10].

The singlet axial current is normalized by introducing a number of flavors N_f as

$$A_\mu^0 = \frac{1}{\sqrt{N_f}}\bar{q}\gamma_\mu\gamma_5 q \quad (2)$$

and the divergence

$$\partial^\mu A_\mu^0 = \sqrt{2N_f}\frac{1}{16\pi^2}tr_c\epsilon^{\alpha\beta\mu\nu}G_{\alpha\beta}G_{\mu\nu} = \sqrt{2N_f}\omega \quad (3)$$

The η' field defined in [5] is

$$\langle 0|A_\mu^0|\eta'\rangle = ip_\mu F_0, \quad \langle 0|\omega|\eta'\rangle = \sqrt{2N_f}\frac{\tau}{F_0}$$

where the mass of η' and the parameter τ are related by

$$M_{\eta'}^2 = \frac{2N_f\tau}{F_0^2} \quad (4)$$

The triangle diagram yields the electromagnetic anomaly of the axial quark charge current

$$\partial_\mu j_\mu^{5\lambda} = -\frac{e^2}{16\pi^2} \epsilon^{\alpha\beta\mu\nu} F_{\alpha\beta} F_{\mu\nu} \cdot \text{tr}[\tau^\lambda Q^2]$$

where $F_{\mu\nu}$ is the electromagnetic field strength,

$$Q = \begin{pmatrix} \frac{2}{3} & 0 \\ 0 & -\frac{1}{3} \end{pmatrix}$$

is the quark electric charge and tr is over colors and flavors[11].

The Nambu-Goldstone boson π 's decay into two gamma rays is described by divergence of the axial current. The Adler-Bardeen[12]'s theorem says that higher-order effects in the triangular diagram of pion decay into two photons can be incorporated in the renormalization

$$\partial_\mu j_\mu^5 = \epsilon^{\alpha\beta\mu\nu} F_{\alpha\beta} F_{\mu\nu} \frac{e_0^2}{8\pi^2} \left(1 - \frac{3e_0^4}{64\pi^4} \log \frac{\Lambda^2}{m^2}\right)$$

The axial anomaly is not exhausted by the single loop, and radiative corrections were evaluated by several authors[13, 14, 15]. Ioffe calculated the divergence of the axial current from the triangle diagram using the gluonic field strength as

$$\partial_\mu j_\mu^{5\lambda} = -\frac{\alpha_s}{4\pi} \epsilon^{\alpha\beta\mu\nu} G_{\alpha\beta} G_{\mu\nu} \cdot N_c$$

where $N_c = 3$ is the number of colors.

The decay process of Nambu-Goldstone boson π^0 can be derived from current algebra and constrained by the symmetry of the vector current, whose triality sector is fixed. The gluons exchanged between the quark triangle, and the quark rectangle would be constrained to be in a triality sector, and the twisted diagram does not contribute. The standard chiral effective theory predicts[14]

$$\Gamma(\pi^0 \rightarrow \gamma\gamma) = \frac{\alpha^2}{32\pi^3} \frac{m_\pi^3}{f_\pi^2} = 7.7\text{eV}.$$

Experimentally, $\Gamma(\pi^0 \rightarrow \gamma\gamma) = 7.82 \pm 0.14 \pm 0.17 \text{eV}$ [16].

Divergence of an isoscalar axial current could play a role in $\eta \rightarrow \gamma\gamma$ and/or $\eta' \rightarrow \gamma\gamma$ decay processes, in which instanton contribute and the twisted diagram appears. A simple theoretical extension of $\pi^0 \rightarrow \gamma\gamma$ to $\eta \rightarrow \gamma\gamma$ predicts[14]

$$\Gamma(\eta \rightarrow \gamma\gamma) = \frac{\alpha^2}{32\pi^3} \frac{1}{3} \frac{m_\eta^3}{f_\eta^2} = 0.13 \text{keV}$$

Experimentally, $\Gamma(\eta \rightarrow \gamma\gamma) = 0.510 \pm 0.026 \text{keV}$ [16] is about 4 times larger.

A simple multiplication of $(m_{\eta'}/m_\eta)^3$ predicts

$$\Gamma(\eta' \rightarrow \gamma\gamma) = \frac{\alpha^2}{32\pi^3} \frac{1}{3} \frac{m_{\eta'}^3}{f_{\eta'}^2} = 0.69 \text{keV}$$

Experimental data of $\Gamma(\eta' \rightarrow \gamma\gamma) = 4.34 \pm 0.14 \text{keV}$ [16] is about six times larger, and the average decay width of η and η' is 5 times larger.

In [17], one loop correction to the Wess-Zumino Lagrangean governing $\pi^0, \eta \rightarrow \gamma\gamma$ decay widths were studied. They used the eighth member of SU(3) octet, η_8 and the SU(3) singlet η_0 as

$$\begin{aligned} |\eta\rangle &= \cos\theta |\eta_8\rangle - \sin\theta |\eta_0\rangle \\ |\eta'\rangle &= \sin\theta |\eta_8\rangle + \cos\theta |\eta_0\rangle \end{aligned} \quad (5)$$

and obtained $\theta \simeq -20^\circ$. Ref. [5, 8] also obtained $\theta = -20^\circ$, but the studies of vacuum using quark-flavor basis rather than the octet-singlet basis turned out to fit data of η, η' better[18, 19].

The one-mixing angle scheme turned out to be valid only in large N_c limit[5, 7, 8]. Bhagwat et al[10] defined the kernel of Bethe-Salpeter equation of pseudoscalar mesons as

$$K = K_L + K_A$$

where K_L is the leading order term and K_A is the term associated with the anomaly, which is parametrized as

$$\begin{aligned} (K_A)_{rs}^{tu}(q, p, P) &= -\xi((q-p)^2) \{ \cos^2\theta_\xi [\zeta \gamma_5]_{rs} [\zeta \gamma_5]_{tu} + \sin^2\theta_\xi [\zeta \gamma \cdot P \gamma_5]_{rs} [\zeta \gamma \cdot P \gamma_5]_{tu} \} \\ \xi(k^2) &= (2\pi)^4 \xi \delta^4(k) \end{aligned} \quad (6)$$

with a dimensionless coupling constant ξ as a parameter, and the quark mass function

$$\zeta = \text{diag}[\frac{1}{M_u^D}, \frac{1}{M_d^D}, \frac{1}{M_s^D}, \dots], \quad M_f^D = M_f(s=0) \quad (7)$$

where f is the quark flavor.

When the basis of non-strange η and strange η ,

$$\begin{aligned} |\eta_{NS}\rangle &= \frac{1}{\sqrt{2}}(|u\bar{u}\rangle + |d\bar{d}\rangle) = \frac{1}{\sqrt{3}}|\eta_8\rangle + \sqrt{\frac{2}{3}}|\eta_0\rangle \\ |\eta_S\rangle &= |s\bar{s}\rangle = -\sqrt{\frac{2}{3}}|\eta_8\rangle + \frac{1}{\sqrt{3}}|\eta_0\rangle \end{aligned} \quad (8)$$

are used,

$$\begin{aligned} |\eta\rangle &= \cos\phi|\eta_{NS}\rangle - \sin\phi|\eta_S\rangle \\ |\eta'\rangle &= \sin\phi|\eta_{NS}\rangle + \cos\phi|\eta_S\rangle. \end{aligned} \quad (9)$$

The experimental value $\phi = 41.88^\circ$ corresponds to $|\eta_{NS}\rangle = 0.427$, $|\eta_S\rangle = 0.0860$, and $\theta = \phi - \arctan\sqrt{2} = \phi - 54.74^\circ = -12.9^\circ$ [9]. When the parameter $\xi = 0.076$ was taken, $\theta_\eta = -15.4^\circ$ and $\theta'_\eta = -15.7^\circ$ were obtained[10].

In a phenomenological model using the quark-flavor basis and assuming mixing angle $\phi_q \simeq \phi_s \sim 40^\circ$, the decay width of η and η' could be fitted[19], and a lattice simulation using the similar bases of (9), and including the loop of c quarks, obtained also $\phi = 46^\circ$ [20].

2 Triality symmetry of É.Cartan

É.Cartan[21] studied algebra of system of spinors and vectors, which have the triality symmetry. He considered in the euclidean space $E_{2\nu}$, the semispinors ϕ which are specified by an even number of indices: $\xi_0, \xi_{23}, \xi_{31}, \xi_{12}, \xi_{1234}, \xi_{14}, \xi_{24}$ and ξ_{34} and semispinors ψ which are specified by an odd number of indices:

The spinor bases A, B, C, D are expressed as

$$\begin{aligned} A &= \xi_{14}\sigma_x + \xi_{24}\sigma_y + \xi_{34}\sigma_z + \xi_0\mathbf{I} \\ B &= \xi_{23}\sigma_x + \xi_{31}\sigma_y + \xi_{12}\sigma_z + \xi_{1234}\mathbf{I} \\ C &= \xi_1\sigma_x + \xi_2\sigma_y + \xi_3\sigma_z + \xi_4\mathbf{I} \\ D &= \xi_{234}\sigma_x + \xi_{314}\sigma_y + \xi_{124}\sigma_z + \xi_{123}\mathbf{I} \end{aligned} \tag{10}$$

and the vector fields are expressed as

$$\begin{aligned} E &= x_1\mathbf{i} + x_2\mathbf{j} + x_3\mathbf{k} + x_4\mathbf{I} \\ E' &= x'_1\mathbf{i} + x'_2\mathbf{j} + x'_3\mathbf{k} + x'_4\mathbf{I}. \end{aligned} \tag{11}$$

The coupling of spinors to vector particles x_i and x'_j are expressed as ${}^t\phi CX\psi$. É. Cartan considered 5 superspace transformations $G_{23}, G_{12}, G_{13}, G_{123}$ and G_{132} . By the transformation G_{12} , the spinor ${}^t(A, B)$ is transformed to E, E' in which the 4th component of the vector field x_4 and x'_4 are interchanged, and E, E' are transformed to ${}^t(A, B)$ in which ξ_{1234} and ξ_0 are interchanged.

The operator G_{23} does not transform vectors to spinors or spinors to vectors, but its operation on Dirac fermions is a charge conjugation,

$$G_{23} \begin{pmatrix} A \\ B \end{pmatrix} = \begin{pmatrix} C \\ D \end{pmatrix}, \quad G_{23} \begin{pmatrix} C \\ D \end{pmatrix} = - \begin{pmatrix} A \\ B \end{pmatrix}.$$

and its operation on vector field E and E' is an interchange of the 4th component.

$$\begin{aligned} G_{23} \begin{pmatrix} E \\ E' \end{pmatrix} &= G_{23} \begin{pmatrix} x_1 \mathbf{i} + x_2 \mathbf{j} + x_3 \mathbf{k} + x_4 \mathbf{I} \\ x'_1 \mathbf{i} + x'_2 \mathbf{j} + x'_3 \mathbf{k} + x'_4 \mathbf{I} \end{pmatrix} \\ &= \begin{pmatrix} x_1 \mathbf{i} + x_2 \mathbf{j} + x_3 \mathbf{k} - x'_4 \mathbf{I} \\ x'_1 \mathbf{i} + x'_2 \mathbf{j} + x'_3 \mathbf{k} - x_4 \mathbf{I} \end{pmatrix}. \end{aligned}$$

When the vector fields are selfdual, and the energy is null, a singular behavior can be expected from $G_{23}E$ and $G_{23}E'$.

When G_{13} operates on left-handed fermion the 4th component of A and B , ξ_0 and ξ_{1234} , respectively are interchanged:

$$\begin{aligned} G_{13} \begin{pmatrix} A \\ B \end{pmatrix} &= G_{13} \begin{pmatrix} \xi_{14}\sigma_x + \xi_{24}\sigma_y + \xi_{34}\sigma_z + \xi_0 \mathbf{I} \\ \xi_{23}\sigma_x + \xi_{31}\sigma_y + \xi_{12}\sigma_z + \xi_{1234} \mathbf{I} \end{pmatrix}, \\ &= \begin{pmatrix} \xi_{14}\sigma_x + \xi_{24}\sigma_y + \xi_{34}\sigma_z + \xi_{1234} \mathbf{I} \\ \xi_{23}\sigma_x + \xi_{31}\sigma_y + \xi_{12}\sigma_z + \xi_0 \mathbf{I} \end{pmatrix}. \\ G_{13} \begin{pmatrix} E \\ E' \end{pmatrix} &= \begin{pmatrix} D \\ C \end{pmatrix} = \begin{pmatrix} \xi_{234}\sigma_x + \xi_{314}\sigma_y + \xi_{124}\sigma_z + \xi_{123} \mathbf{I} \\ \xi_1\sigma_x + \xi_2\sigma_y + \xi_3\sigma_z + \xi_4 \mathbf{I} \end{pmatrix} \end{aligned}$$

In quantum electrodynamics, the success of Dirac spinors which are described by quaternions is established, but in QCD, it is not so evident. I study in this paper, consequences of the interchange of the 4th component in the octonion by extending the QCD using octonions. The QCD in quaternion basis was studied in [22, 23, 24, 25, 26], and recently, I discussed the axial anomaly using octonion bases and considered rescattering diagrams in [27].

The vector particles that propagate between the triangle diagram and the square diagram can be photons as well as gluons. In low energy, the effect of gluons is expected to be important, but transition from two gluons to two photons via square diagram or the gluon and photon scattering at low energy is not well understood[28].

In the rescattering diagram, I considered the change of vector particles x_i and x_j to x'_i and x'_j without changing the polarization direction.

In chiral gauge theory, left-handed quarks and left-handed leptons are defined as

$$Q_L = \begin{pmatrix} u \\ d \end{pmatrix} \quad L_L = \begin{pmatrix} \nu \\ l \end{pmatrix}$$

and right-handed leptons Ψ_R are defined as

$$\Psi'_{L_i} = \sigma^2 \Psi_{R_i}^* \quad \Psi'^{\dagger}_{L_i} = \Psi_{R_i}^T \sigma^2$$

The left-handed fermion ${}^t(A, B)$ is defined as a fermion and its right-handed anti-particle (C, D) is defined as a new right-handed fermion.

The fermionic Lagrangian in the standard model is

$$\mathcal{L} = \bar{\Psi} i \gamma^\mu \left(\partial_\mu - ig A_\mu^a t_r^a \left(\frac{1 - \gamma^5}{2} \right) \right) \Psi$$

In É. Cartan's convention, the projection operator $\frac{1 - \gamma^5}{2}$ is contained in ϕ or ψ and

$$\bar{\Psi} = (\phi, \psi) \begin{pmatrix} 0 & 1 \\ 1 & 0 \end{pmatrix} = (\psi, \phi)$$

Quarks and leptons belong to their triality sectors, and I assume that the electromagnetic interaction has the triality selection rules, or electron e , muon μ and tauon τ react to quarks in their same triality sector. Quarks may emit photons in an arbitrary triality sector, but if photons from quarks in the triality sector different from that of leptons are not detected, and if $\mu \rightarrow e\gamma$ is not observed, (its actual experimental probability is less than 10^{-11}), the triality selection rule can be established.

The vector field E and E' of É. Cartan is a kind of generalization of the electro magnetic field A_μ . When a pair of vector particles E, E or $E' E'$ transform into a quark-antiquark pair and return to two same type of vectors E, E or E', E' , we call the diagram a rescattering diagram. The quark-antiquark system may have isospin 1, like π . When different types E, E' transform into a quark-antiquark pair and return to E, E' , we call the diagram a twisted diagram. The corresponding quark-antiquark systems have isospin 0, like η and η' .

3 Rescattering diagrams

Due to the γ_5 operator in the axial vector vertex, the triangle diagram introduces an operator containing 4 components $\partial_i, x_j, \partial_k$ and x_m , combined by the anti-commutation factor ϵ_{ijkm} . Emitted two vector particles can be absorbed by a fermion, and the fermion can emit two vector particles. When the polarizations of the two vector particles do not change in the two emissions, I call the diagram as a rescattering diagram.

In QED, a e_0^6 term appears from rescattering of two photons of two different polarizations, as shown in Figs.1-8. They contain square diagrams contoured by four quark lines. In Figs.1-4, axial vector current couples to fermions with an even number of indices, and In Figs.5-8, it couples to fermions with an odd number of indices.

I choose the propagator between two vector particles emission points in the $A_1 x_2 x_3$ or $A_1 x'_2 x'_3$ diagram and between the final $x'_2 x'_3$ or $x_2 x_3$ emission points to be spinless. In this model, the $A_1(A'_1)\sigma_x$ vertex is produced from the product:

$$\xi_{12}\sigma_z \times \xi_{31}\sigma_y \rightarrow -A_1\sigma_x, \xi_{34}\sigma_z \times \xi_{24}\sigma_y \rightarrow -A_1\sigma_x, \xi_3\sigma_z \times \xi_2\sigma_y \rightarrow -A'_1\sigma_x$$

and $\xi_{124}\sigma_z \times \xi_{314}\sigma_y \rightarrow -A'_1\sigma_x$.

Similarly, $A_2(A'_2)\sigma_y$ vertex is produced from the product:

$$\xi_{23}\sigma_x \times \xi_{12}\sigma_z \rightarrow -A'_2\sigma_y, \xi_{14}\sigma_x \times \xi_{34}\sigma_z \rightarrow -A'_2\sigma_y, \xi_1\sigma_x \times \xi_3\sigma_z \rightarrow -A_2\sigma_y$$

and $\xi_{124}\sigma_z \times \xi_{234}\sigma_x \rightarrow A_2\sigma_y$

Similarly, $A_3(A'_3)\sigma_z$ vertex is produced from the product:

$$\xi_{31}\sigma_y \times \xi_{23}\sigma_x \rightarrow -A'_3\sigma_z, \xi_{24}\sigma_y \times \xi_{14}\sigma_x \rightarrow -A'_3\sigma_z, \xi_2\sigma_y \times \xi_1\sigma_x \rightarrow -A_3\sigma_z$$

and $\xi_{314}\sigma_y \times \xi_{234}\sigma_x \rightarrow -A_3\sigma_z$

The amplitude that includes the half circle of Fig.1 and Fig.2 is

$$\begin{aligned} T'_{321}(k, q) &= -e^2 \int \frac{d^4 p}{(2\pi)^4} Tr[\gamma_3 \frac{1}{p - (k - q) - m} \gamma_1 \gamma_5 \frac{1}{p - q - m} \gamma_2 \frac{1}{p - k - m}] \\ &\propto G'_{3\sigma}(k) G'_{2\rho}(q) \epsilon^{3\sigma 2\rho} \end{aligned} \quad (12)$$

where $G'_{\lambda\mu}(k) = k_\lambda x'_\mu - k_\mu x'_\lambda$, and $\epsilon^{3124} = 1$ and $\epsilon^{3421} = -1$.

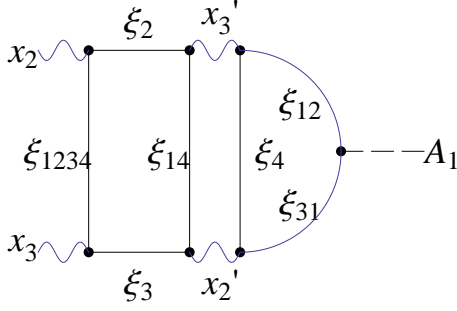


Figure 1: The half circle diagram of an axial anomaly. $A_1 x'_3 x'_2$ type and its rescattering.

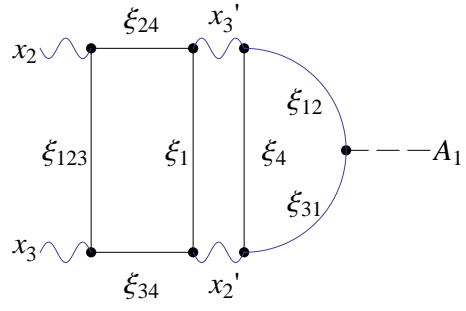


Figure 2: The half circle diagram of an axial anomaly. $A_1 x'_3 x'_2$ type and its rescattering.

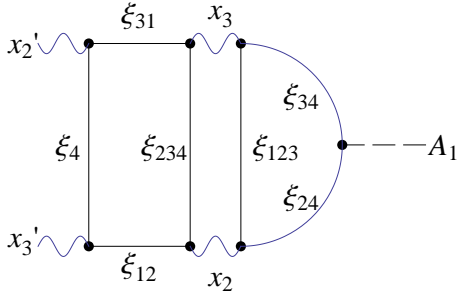


Figure 3: $A_1 x_3 x_2$ type and its rescattering.

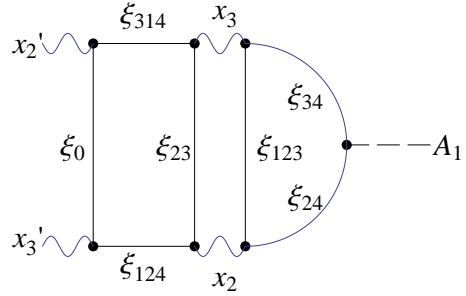


Figure 4: $A_1 x_2 x_3$ type and its rescattering.

The amplitude that includes the half circle of Fig.3 and Fig.4 is

$$T_{321}(k, q) \propto G_{3\sigma}(k) G_{2\rho}(q) \epsilon^{3\sigma 2\rho}$$

where $G_{\lambda\mu}(k) = k_\lambda x_\mu - k_\mu x_\lambda$.

4 Twisted diagrams

When the vector particles are self-dual, there is no reason to restrict an emission of two vector particles in the triangle diagram to be of type $x_i x_j$ or $x'_i x'_j$. When the emitted vector particles are $x_4 x'_i$ or $x'_4 x_i$, where $i = 1, 2, 3$, the fermion square diagram can emit two vector particles $x_j x'_k$ or $x'_j x_k$ where $j \neq k$ and they are not equal to $'i'$ and $'4'$. When the emitted vector particles are $x'_2 x_3$ or $x_2 x'_3$, the fermion square can emit $x_1 x'_4$ or $x'_1 x_4$, respectively.

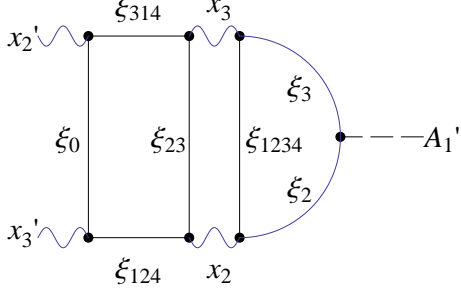


Figure 5: $A'_1 x_3 x_2$ type and its rescattering.

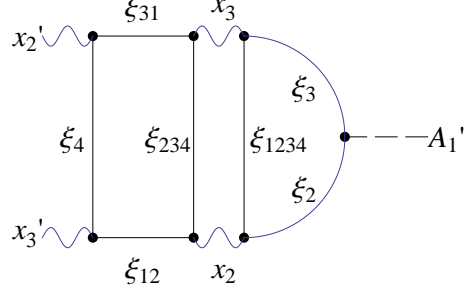


Figure 6: $A'_1 x_2 x_3$ type and its rescattering.

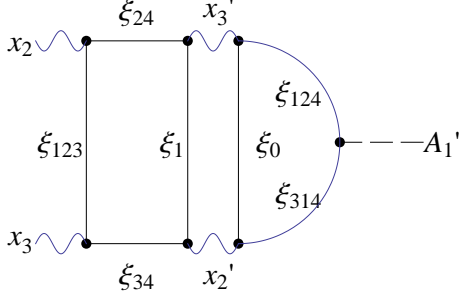


Figure 7: $A'_1 x'_3 x'_2$ type and its rescattering.

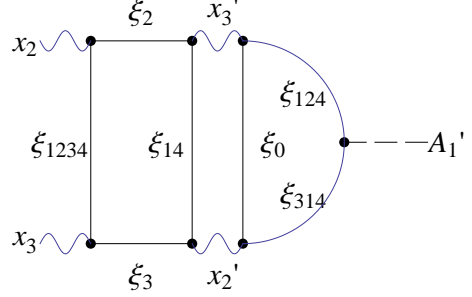


Figure 8: $A'_1 x'_2 x'_3$ type and its rescattering.

When the vector fields can be treated as self-dual, i.e. x_i and x'_j interact with ξ_{1234} and ξ_0 , one could consider topologically complicated processes in which after twice rotations, (the first via ξ_{1234} and the second via ξ_0) the initial configuration reappears.

G_{13} transforms $(A_1, A_2, A_3, A_4) \rightarrow (A_1, A_2, A_3, B_4)$ and $(B_1, B_2, B_3, B_4) \rightarrow (B_1, B_2, B_3, A_4)$. In other words, ξ_{1234} is replaced by ξ_0 . Since the intermediate quark propagator that absorbs and emits $x_1 x'_4$ or $x_4 x'_1$ is not expected to be in the eigenstate of G_{13} , the quark ξ_{123} that absorbs x'_4 is transformed to ξ_0 but through the mixed component of ξ_{1234} , it will emit x_1 and changes to ξ_1 as shown in Fig.9.

When vector particles are selfdual and x_i and x'_i are indistinguishable, the square in the left hand side of Fig.9 and Fig.10 give an amplitude, in which a spinor ξ_a emits a vector particle x_b and changes to a spinor ξ_c is represented as ξ_a, x_b, ξ_c , of the type

$$(\xi_{1234}, x'_4), \xi_1, x'_3, \xi_{24}, x_2, \xi_{123}, x'_4, \xi_0, x_1,$$

$$(\xi_0, x_1), \xi_{123}, x_3, \xi_{34}, x'_2, \xi_1, x_1, \xi_{1234}, x'_4.$$

They emit x_2, x'_2 and x_3, x'_3 but do not contain x_4 and x'_1 .

They are included in the amplitudes

$$T_{3241}(K, Q, q, k) \propto G'_{3\rho}(K)G_{2\tau}(Q)G_{4v}(q)'G_{1\sigma}(k)\epsilon^{3\rho 2\tau}\epsilon^{4v 1\sigma}$$

$$T_{3214}(K, Q, k, q) \propto G_{3\rho}(K)G'_{2\tau}(Q)G_{1\sigma}(k)G'_{4v}(q)\epsilon^{3\rho 2\tau}\epsilon^{1\sigma 4v}.$$

The amplitude that includes the right hand loop of Fig.9 and Fig.10 are

$$\begin{aligned} T''_{41}(k, q) &\propto G'_{4\bar{v}}(q)G_{1\bar{\sigma}}(k)\epsilon^{4\bar{v} 1\bar{\sigma}} \\ T'''_{14}(k, q) &\propto G'_{1\bar{\sigma}}(k)G_{4\bar{v}}(q)\epsilon^{1\bar{\sigma} 4\bar{v}}. \end{aligned} \quad (13)$$

They are included in the amplitudes

$$\begin{aligned} T_{324141\mu}(K, Q, q, k) &= -e^2 g^4 \int \frac{d^4 p}{(2\pi)^4} \int \frac{d^4 P}{(2\pi)^4} Tr[\gamma_3 \frac{1}{(P+K)-m} \gamma_2 \frac{1}{(P+K+Q)-m} \\ &\quad \times \gamma_1 \frac{1}{P-m} \gamma_4 \frac{1}{(P+k)-m}] \frac{1}{k^2 + \epsilon} \frac{1}{q^2 + \epsilon} \delta(P+K+Q-p-k-q) \\ &\quad \times Tr[\gamma_4 \frac{1}{(p-k+q)-m} \gamma_\mu \gamma_5 \frac{1}{p-m} \gamma_1 \frac{1}{(p-k)-m}] \\ &\propto G'_{3\rho}(K)G_{2\tau}(Q)G'_{4v}(q)G_{1\sigma}(k)\epsilon^{3\rho 2\tau}\epsilon^{4v 1\sigma} G'_{4\bar{v}}(q)G_{1\bar{\sigma}}(k)\epsilon^{4\bar{v} 1\bar{\sigma}} \\ &\propto G'_{3\rho}(K)G_{2\tau}(Q)\epsilon^{3\rho 2\tau}(G'_{43}(q)G_{12}(k) - G'_{42}(q)G_{13}(k))^2 \\ T_{321414\mu}(K, Q, k, q) &= -e^2 g^4 \int \frac{d^4 p}{(2\pi)^4} \int \frac{d^4 P}{(2\pi)^4} Tr[\gamma_3 \frac{1}{(P+K)-m} \gamma_2 \frac{1}{(P+K+Q)-m} \\ &\quad \times \gamma_1 \frac{1}{P-m} \gamma_4 \frac{1}{(P+q)-m}] \frac{1}{k^2 + \epsilon} \frac{1}{q^2 + \epsilon} \delta(P+K+Q-p-q-k) \\ &\quad \times Tr[\gamma_4 \frac{1}{(p-q+k)-m} \gamma_\mu \gamma_5 \frac{1}{p-m} \gamma_1 \frac{1}{(p-q)-m}] \\ &\propto G_{3\rho}(K)G'_{2\tau}(Q)G_{1\sigma}(k)G'_{4v}(q)\epsilon^{3\rho 2\tau}\epsilon^{1\sigma 4v} G_{1\bar{\sigma}}(k)G'_{4\bar{v}}(q)\epsilon^{1\bar{\sigma} 4\bar{v}} \\ &\propto G_{3\rho}(K)G'_{2\tau}(Q)\epsilon^{3\rho 2\tau}(G_{13}(k)G'_{42}(q) - G_{12}(k)G'_{43}(q))^2 \end{aligned}$$

In Figs.9-16, the quark spinor $\xi_{1234}I$ absorbs vectors x_i , the spinor $\xi_0 I$ absorbs x'_i . Gluons polarized in the four directions x'_1, x'_2, x_3, x_4 , x_1, x_2, x'_3, x'_4 or x'_1, x_2, x'_3, x_4 (and x_i, x'_i interchanged) appear on the twisted diagrams.

The vector x_4 and x'_1 have common coupling to spinor ξ_{123} and ξ_1 . In Fig.9, the product $\xi_1\sigma_x \times \xi_{24}\sigma_y \rightarrow x'_3\mathbf{k}$ and $\xi_{24}\sigma_y \times \xi_{123}I \rightarrow x_2\mathbf{j}$ the final two vectors $x'_3\mathbf{k} \times x_2\mathbf{j}$ makes a vector product $-x_1\mathbf{i}$. After emission of x_2 , ξ_{123} emits a x'_4 and becomes ξ_0 , and as shown in Fig.10, absorbs x'_4 and becomes ξ_{123} . It emits x_3 and x'_2 and becomes ξ_1 . It emits x_1 and goes to ξ_{1234} . ξ_{1234} absorbs x_1 as shown in Fig.9 and emits x'_3 and x_2 and returns to ξ_{123} . In Fig.11 and Fig.12, the spinor ξ_{123} is replaced by ξ_1 .

The relative sign of $x'_3\mathbf{k} \times x_2\mathbf{j}$ from Fig.9 and $x'_2\mathbf{j} \times x_3\mathbf{k}$ from Fig.10 is cancelled by the relative sign of the product of 6 vertices $\xi_*x_j\xi_{*'}'$, where j runs from 1 to 4, and $\xi_*, \xi_{*'}'$ run $\xi_\alpha, \xi_{\alpha\beta}, \xi_{\alpha\beta\gamma}$ or ξ_{1234} that appear on the Figures.

The vector x'_4 and x_1 have the common coupling to spinor ξ_{234} and ξ_4 . In Figs. 13-16, the same mechanism occurs as in Figs.9-12, in which ξ_{123} is replaced by ξ_{234} and ξ_1 is replaced by ξ_4 .

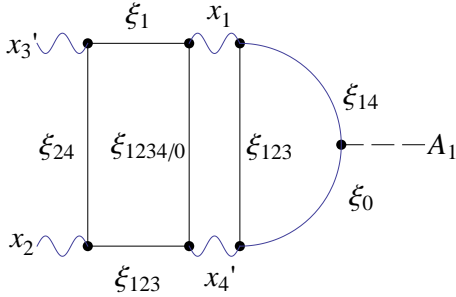


Figure 9: The axial anomaly diagram via $A_1x_1x'_4$ to $A_1x'_3x_2$.

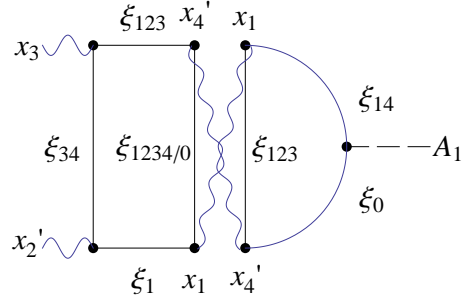


Figure 10: The axial anomaly diagram via $A_1x_1x'_4$ to $A_1x_3x'_2$.

Diagrams for vertices via $A_2x_2x'_4$ to $A_2x'_1x_3$, etc. and via $A_3x_3x'_4$ to $A_3x_1x'_2$, etc. are similar.

In Figs.17-24, I show the cases of the vector particles x_1/x'_1 and x'_4/x_4 in the final state. In Figs.17-18, the quark propagator between x'_2 and x_3 is ξ_{314} on the side of A_1 vertex, but ξ_{1234} or ξ_0 on the side of $x_1x'_4$. ξ_{1234} and ξ_0 are the 4th component of spinor B and A , respectively. When G_{13} operates on ${}^t(A, B)$, ξ_{1234} and ξ_0 are interchanged. Therefore, a

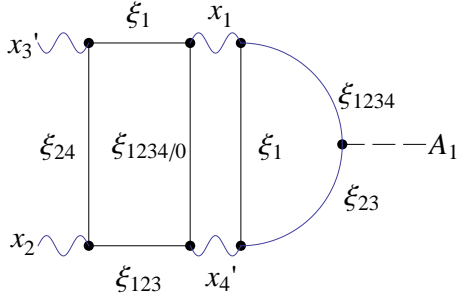


Figure 11: The diagram via $A_1 x_1 x_4'$ to $A_1 x_3' x_2$.

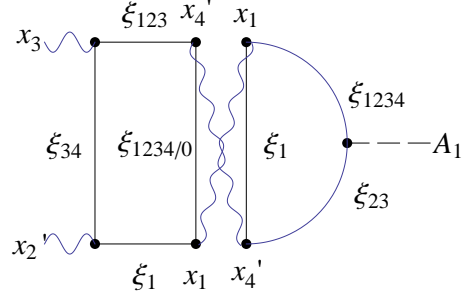


Figure 12: The diagram via $A_1 x_1 x_4'$ to $A_1 x_3 x_2'$.

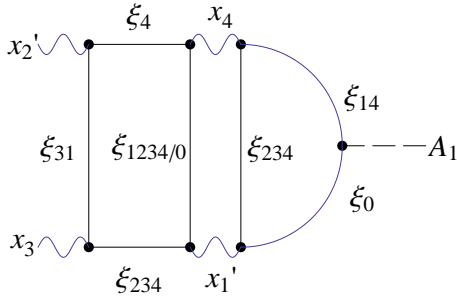


Figure 13: The diagram via $A_1 x_4 x_1'$ to $A_1 x_2' x_3$.

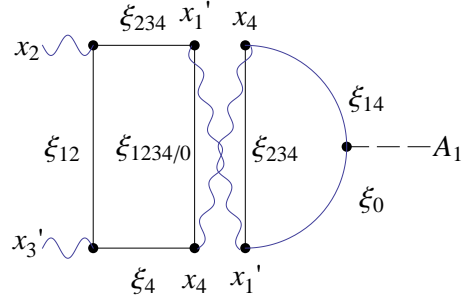


Figure 14: The diagram via $A_1 x_4 x_1'$ to $A_1 x_2 x_3'$.

mixing of ξ_{1234} and ξ_0 inside the quark loop occur.

The Fig.17 and Fig.18 are contained in the amplitude

$$T_{1432}(K, Q, k, q) \propto G_{1\rho}(K) G'_{4\tau}(Q) G_{3v}(k) G'_{2\sigma}(q) \epsilon^{1\rho 4\tau} \epsilon^{3v 2\sigma}$$

$$T_{1423}(K, Q, q, k) \propto G'_{1\rho}(K) G_{4\tau}(Q) G'_{2\sigma}(q) G_{3v}(k) \epsilon^{1\rho 4\tau} \epsilon^{2\sigma 3v}.$$

Mixing of ξ_{1234} and ξ_0 is important. Experimentally, $x_1' x_4$ or $x_1 x_4'$ state will not be detected, but via rescattering it changes to $x_2' x_3$ or $x_2 x_3'$ state.

The diagrams for $A_2 x_1' x_3$, $A_2 x_1 x_3'$ and $A_3 x_2' x_1$, $A_3 x_2 x_1'$ are similar.

In the twisted diagrams, a mixing of ξ_{1234} and ξ_0 is assumed, which appears after transformations of G_{12} , G_{13} , G_{123} and G_{132} . The two vector particles which appear on the triangle diagram belong to different groups E and E' , respectively. Such processes would contribute

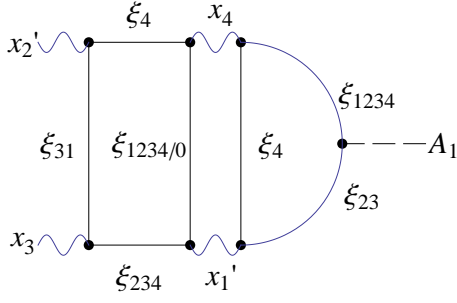


Figure 15: The diagram via $A_1 x_4 x_1'$ to $A_1 x_2' x_3$.

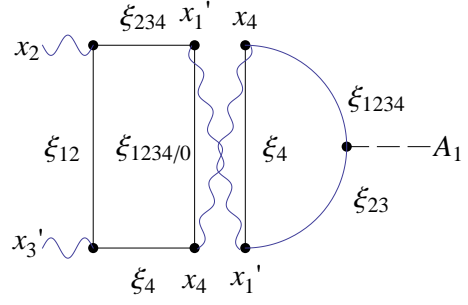


Figure 16: The diagram via $A_1 x_4 x_1'$ to $A_1 x_2 x_3'$.

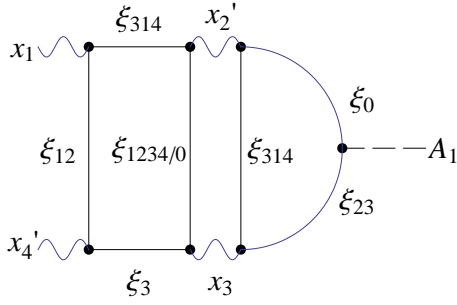


Figure 17: The diagram via $A_1 x_2' x_3$ to $A_1 x_1 x_4'$.

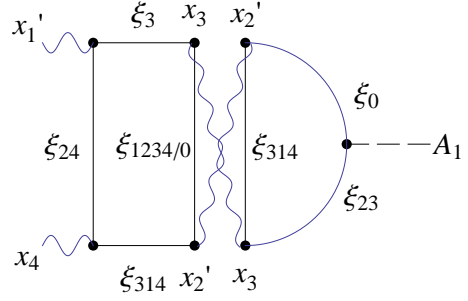


Figure 18: The diagram via $A_1 x_2' x_3$ to $A_1 x_1' x_4$.

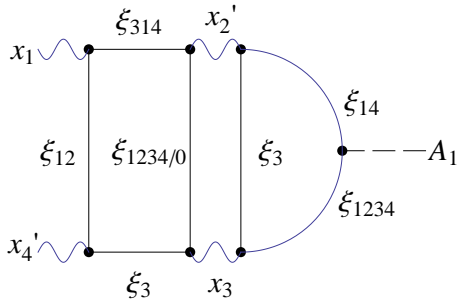


Figure 19: The diagram via $A_1 x_2' x_3$ to $A_1 x_1 x_4'$.

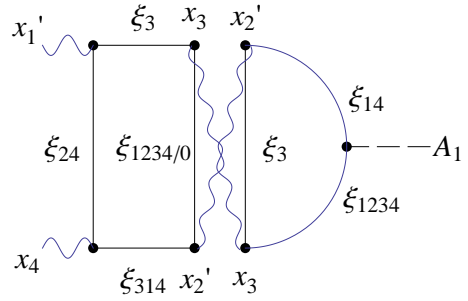


Figure 20: The diagram via $A_1 x_2' x_3$ to $A_1 x_1' x_4$.

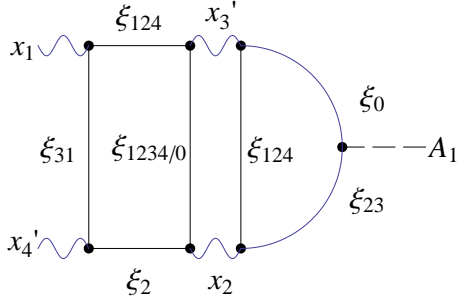


Figure 21: The diagram via $A_1 x'_3 x_2$ to $A_1 x_1 x'_4$.

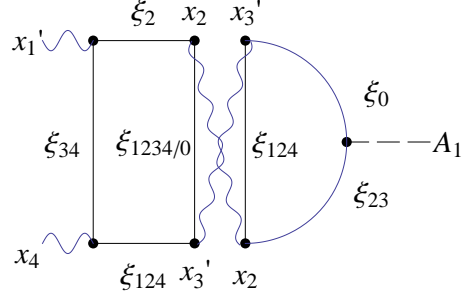


Figure 22: The diagram via $A_1 x'_3 x_2$ to $A_1 x'_1 x_4$.

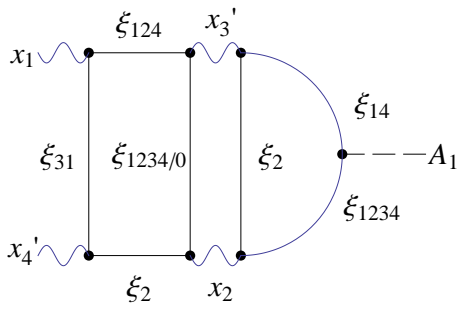


Figure 23: The diagram via $A_1 x'_3 x_2$ to $A_1 x_1 x'_4$.

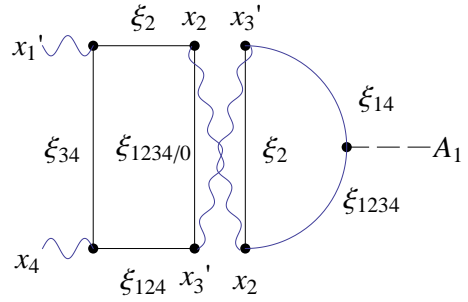


Figure 24: The diagram via $A_1 x'_3 x_2$ to $A_1 x'_1 x_4$.

in the instanton and do not enter in decays of a Nambu-Goldstone boson.

A possible origin of large ϕ is a contribution of the twisted diagram, in which the 4th component of the quark that runs on the loop becomes a mixed state due to the operation of G_{13} in the transition to the intermediate state.

5 Discussion and Conclusion

Whether É. Cartan's spinor matches the dynamics of QCD is not trivial. However, if physical theories are assembly of mathematical models or assembly of rules that connect elements of models and observables[1], there is a possibility that the triality symmetry plays a role in QCD. The possible role of the triality property of $SO(8)$ group in the quark system was discussed in [29]. In my model, the triality selection rule in the electromagnetic interaction of leptons was incorporated, and no selection rule was assumed in the interaction of quarks.

Photons emitted from matter made of quarks that belong to a triality sector different from that of electromagnetic probes, will not be detected, and the matter will be assigned as a dark matter. Dark matter search is done by the Xenon100 detector[30], and a direct detection of composite dark matter through lattice calculation of electromagnetic form factors and comparison to the data of Xenon100 was proposed[31]. The dark matter with masses less than 10TeV was excluded in this analysis. However, the detection through electromagnetic probes in our world would be impossible due to the triality selection rule.

The dark matter search was done also in AMS-02 by measuring positron fraction in cosmic rays[32]. The signal that is detected in our electromagnetic probe would not originate from dark matter, but rather from pulsars, as a recent analysis suggests[33].

A comparison of the decay width of $\eta \rightarrow \gamma\gamma$ and $\eta' \rightarrow \gamma\gamma$ could be a place to study the effect of triality symmetry, including η or η' decay into intermediate two vector particles in twisted diagrams. An investigation of the photon-gluon scattering contribution to the structure functions of deep inelastic scattering for unpolarized as well as polarized photons

and gluons[28] could provide helpful information. The Primakoff production of η and η' in the Coulomb field of a nucleon also shows enhancement as compared to the production of π mesons[34, 35, 36, 37].

In [26], I considered three massless neutrinos in different triality sectors interacting with each other and produced one heavy and two degenerate light neutrinos. ν_e, ν_μ and ν_τ have their lepton partners. I expect e, μ and τ are sensitive to flavors, but blind to the triality of neutrinos, quarks and gluons, and that they are sensitive to the triality of electromagnetic waves. If electromagnetic waves from different triality sectors cannot be detected by electromagnetic probes in our world, we can understand the presence of dark matter.

In the rescattering or twisted diagrams, $\bar{q}q$ state that decay into two vector particles appears. Brodsky and Shrock [38, 39] discuss problems in the expectation value of $\bar{q}q$ in QCD, which gives too large cosmological constant Ω_Λ , and claimed that Ω_Λ has the spacial support within hadrons. The recent review [40] explains the region of matter distribution reachable with terrestrial facilities. Whether the spacial support and the region where the triality sector agrees with that of our electromagnetic probes could match is under investigation.

Acknowledgement

The author thanks Craig Roberts for sending helpful references and Stan Brodsky for helpful information and comments.

Appendix: Conjecture on the struture of the vacuum of universe

In order to obtain physical quantities like decay width of π, η and η' mesons, it is necessary to regularize Feynmann integral. Lüscher[41] started from the space-time lattice

$$\Lambda = \{x \in \mathbf{Z}^4 \mid -L/2 < x_\mu \leq L/2, \mu = 1, 2, 3, 4\}$$

and link variables $U(x, \mu)$ defined, when $x \in \Lambda$ and $x + \hat{\mu} \in \Lambda$. The gauge transformation $g(x)$ of the gauge group \mathcal{G} acts on the gauge field \mathcal{U} , and the compact Lie group \mathcal{G} acts in a differential manner on the field manifold \mathcal{F} ,

$$g \in \mathcal{G}, \quad U \in \mathcal{F} \rightarrow g \cdot U = U^g \in \mathcal{F}$$

The orbit manifold $\mathcal{M} = \mathcal{F}/\mathcal{G}$ is a differential manifold and with some measure on \mathcal{F} defined as $d\mu(U)$ and some integrable function defined as $f(U)$, one introduces notations as follows.

We define basis of the Lie algebra \mathcal{L}_G of \mathcal{G} as $T^a, a = 1, \dots, d_G$, general element of \mathcal{L}_G as $X = X_a T^a$ and for any differential function $F(U)$ on \mathcal{F}

$$\delta_X F(U) = X_a \left\{ \frac{\partial}{\partial Y_a} F(e^{-Y} \cdot U) \right\}_{Y=0},$$

is defined.

For any subset of \mathcal{F} , defined as \mathcal{N} , a set

$$[\mathcal{N}] = \{U \in \mathcal{F} \mid g \cdot U \in \mathcal{N} \text{ for some } g \in \mathcal{G}\}$$

is defined as a union of all gauge orbits passing through \mathcal{N} .

It was shown in [41] that, by using invariant measure dg on \mathcal{G} ,

$$\chi(U) = \begin{cases} 1 & \text{if } U \in \mathcal{N}, \\ 0 & \text{otherwise} \end{cases}$$

and the linear operator

$$L(U) \cdot X = \delta_X F(U) \quad \text{for all } X \in \mathcal{L}_G,$$

one can consider for a set $h \in \mathcal{G}$ and $g = e^{-X}h$, a gauge fixing function

$$F(g \cdot U) = L(h \cdot U) \cdot X + O(X^2).$$

For any function $f(U)$ supported in \mathcal{N} , the integral

$$\int_{\mathcal{F}} d\mu(U) f(U) \sim \int_{\mathcal{F}} d\mu(U) f(U) \int_{\mathcal{G}} dg \chi(g \cdot U) \det L(g \cdot U) \delta(F(g \cdot U))$$

reduces in the neighbourhood of h to

$$K \int_{\mathcal{F}} d\mu(U) f(U) \det L(U) \delta(F(U))$$

where K is a constant independent of f .

We consider the vacuum near \mathcal{N} of our universe, and the universe transformed by $G_{23}, G_{12}, G_{13}, G_{123}$ and G_{132} .

References

- [1] Hawking, S. and Mlodinow, L. *The Grand Design*, translated by Sato, K., Kohdansha-pub. (2011).
- [2] Gasser, J. and Leutwyler, H.: Chiral Perturbation Theory: Expansions in the Mass of the Strange Quark, Nucl. Phys. **B250**(1984), 465.
- [3] Wess, J. and Zumino, B.: Consequences of Anomalous Ward Identities, Phys. Lett. **B37**(1971), 95.
- [4] Witten, E.: Global Aspects of Current Algebra, Nucl. Phys. **B223**(1983), 422.
- [5] Keiser, R. and Leutwyler, H.: Large N_c in chiral perturbation theory, Eur. Phys. J. **C17**(2000), 623, arXiv: 0007101[hep-ph].
- [6] Borasoy, B. and Wetzel, S.: U(3) chiral perturbation theory with infrared regularization, Phys. Rev. **D63**(2001), 074019.

- [7] Beisert, N. and Borasoy, B. : $\eta - \eta'$ mixing in U(3) chiral perturbation theory, Eur. Phys. J. **A11** (2001), 329: arXiv: 0107175 v1[hep-ph]
- [8] Borasoy, B. and Nissler, R. : Two-photon decays of π^0, η and η' , Eur. Phys. J. **19** (2004), 367, arXiv: 0309011v2 [hep-ph]
- [9] Kekez, D. and Kabucar, D. : η and η' mesons and dimension 2 gluon condensates $\langle A^2 \rangle$, Phys. Rev. D **73**(2006) 036002.
- [10] Bhagwat, M.S., Chang, L., Liu, Y-X, Roberts, C.D. and Tandy, P.C. : Flavour symmetry breaking and meson masses, Phys. Rev. C **76** (2007), 045203.
- [11] Peskin, M.E. and Schroeder, D.V.: *An Introduction to Quantum Field Theory*, Perseus Books (1995).
- [12] Adler, S.L. and Bardeen, W.A. : Absence of Higher-Order Corrections in the Anomalous Axial-Vector Divergence Equation, Phys. Rev. **182**, 1517 (1969).
- [13] Ansel'm, A.A. and Iogansen, A.A.: Radiative correction to the axial anomaly, JETP Lett. **49**, 214 (1989).
- [14] Ioffe, B.L.: Axial anomaly: the modern status, arXiv:0611026[hep-ph].
- [15] Ioffe, B.L.: Axial anomaly in quantum electro- and chromodynamics and the structure of the vacuum in quantum chromodynamics, Usp.Fiz.Nauk 178:647(2008), arXiv:0809.0212[hep-ph]
- [16] Beringer, J. et al (Particle Data Group): Review of Particle Physics, Phys. Rev. D **86**(2012), 010001.
- [17] Donoghue, J.L., Holstein, B.R. and Lin, Y.-C.: Chiral Loops in $\pi^0, \eta^0 \rightarrow \gamma\gamma$ and $\eta - \eta'$ Mixing, Phys. Rev. Lett. **55** (1985) 2766.

- [18] Shore, G.M. : $\eta'(\eta) \rightarrow \gamma\gamma$: A Tale of Two Anomalies, Phys. Scripta T99 (2002), 84 ,
arXiv:[hep-ph/011165v1]
- [19] Escribano, R. and Frère, J-M. : Study of the $\eta - \eta'$ system in two mixing angle scheme.
JHEP 0506:029,2005: arXiv:0501072 v2[hep-ph]
- [20] Michael, C., Ottnad, K. and Urbach, C. : η and η' mixing from Lattice QCD,
arXiv:1310.1207v2[hep-lat].
- [21] Cartan,É. *The theory of Spinors*,p.118, Dover, New York (1966).
- [22] Furui, S.: Chiral Symmetry and BRST Symmetry Breaking, Quaternion Reality and
Lattice Simulation, *Strong Coupling Gauge Theory in LHC Era*, p.398-400, World Sci-
entific, Singapore (2011).
- [23] Furui, S.: Domain Wall Fermion Lattice Simulation in Quaternion Basis, *The IX
international Conference on Quark Confinement and the Hadron Spectrum-QCHS
IX*, ed by Llanes-Estrada and Pelaéz, AIP Conference Proceedigs 1343, p.533(2011),
arXiv:0912.5397[hep-lat]
- [24] Furui,S.:Fermion flavors in quaternion basis and infrared QCD, Few Body Syst.
52(2012), 171.
- [25] Furui,S.: The magnetic mass of transverse gluon, the B-meson weak decay vertex and
the triality symmetry of octonion, Few Body Syst.**53**(2012), 343.
- [26] Furui,S.:The flavor symmetry in the standard model and the triality symmetry, Int. J.
Mod. Phys. **A27**(2012), 1250158.
- [27] Furui,S.:Axial anomaly and triality symmetry of octonion, Few Body Syst. **54**(2013),
2097, arXiv:1301.2095[hep-ph].

- [28] Bass,S.D., Ioffe,B.L., Nikolaev, N.N. and Thomas,A.W.: On the Infrared Contribution to the Photon-Gluon Scattering and the Proton Spin Content, J. Moscow. Phys. Soc. **1**(1991), 317.
- [29] Silagadze,Z.K.:SO(8) Colour as possible origin of generations,Yad.Fiz. 58 N8:1513-1517 (1995), arXiv:9411381[hep-ph].
- [30] Aprile,E. et al (XENON100 Collaboration): The XENON100 Dark Matter Experiment, Astropart. Phys. 35(2012), 573, arXiv:1107.2155[astro-ph.IM].
- [31] Appelquist,T. et al (LSD Collaboration): Lattice calculation of composite dark matter form factors, arXiv:1201.1693[hep-ph].
- [32] Aguilar, M. et al.: First Results from the Alpha Magnetic Spectrometer on the International Space Station: Precision Measurement of thePositron Fraction in Primary Cosmic Rays of 0.5-350 GeV, Phys. Rev. Lett.**110** (2013), 141102.
- [33] Yuan,Q. et al.: Implication of the AMS-02 positron fraction in cosmic rays, arXiv:1304.1482[astro-ph.HE]
- [34] Browman,A. et al. : Radiative Width of the η Meson, Phys. Rev. Lett.**32**(1974), 1067.
- [35] Browman,A. et al. : Decay Width of the Neutral π Meson, Phys. Rev. Lett.**33**(1974), 1400.
- [36] Latin, I. et al., (PrimEx Collaboration): New Measurement of the π^0 Radiative Decay Width, Phys. Rev. Lett.**106** (2011), 162303.
- [37] Kaskulov, M.M. and Mosel, U. : Primakoff production of π^0, η and η' in the Coulomb field of a nucleus, Phys. Rev. C**84** (2011),065206, arXiv:1103.2097v2[nucl-th].
- [38] Brodsky,S.J. and Shrock,R.: On Condensates in Strongly coupled Gauge Theories, Proc. Nat. Acad. Sci **108** (2011), 45-50, arXiv:0803.2541[hep-th].

- [39] Brodsky,S.J. and Shrock,R.: Standard-Model Condensates and the Cosmological Constant, Proc. Nat. Acad. Sci **108** (2011), 45-50, arXiv:0803.2554[hep-th].
- [40] Cloët, I.C. and Roberts, C.D.: Explanation and Prediction of Observables using Continuum Strong QCD, arXiv:1310.2651[nucl-th]
- [41] Lüscher,M. :Selected Topics in Lattice Field Theory, E. Brezin and J. Zinn-Justin, eds., Les Houches, Session XLIX, 1988, Fields, Strings and Critical Phenomena, Elsevier (1989).